

Ion beam and discharge characteristics of cold cathode ion source

A Atta^{a,b*}, H M Abdel-Hamid^{b,c}, Y H A Fawzy^b & M M El-Okr^d

^aPhysics Department, College of Science, Jouf University, Sakaka, P.O. Box 2014, Saudi Arabia

^bRadiation Physics Department, National Center for Radiation Research and Technology
(NCRRT), Atomic Energy Authority (AEA), Cairo, Egypt

^cDiagnostic Radiology Department, Applied Medical Sciences Faculty, Jazan University, Jazan, 82911, KSA

^dPhysics Department, Faculty of Science, Al-Azhar University, Cairo, Egypt

Received 10 June 2019; accepted 2 December 2019

In this work, some developments in the acceleration system of cold cathode ion source have been constructed to produce broad beam to be used in different industrial applications. An electrostatic probe with electrical circuit is constructed for study the extracted ion beam distribution. Broad beam 25 mm with ion current in the range of 1 mA is extracted from the constructed extraction system. The obtained optimum distance between the extraction grid and acceleration grid is 3 mm. The characteristics are measured to investigate the ion beam current I_b as a function of different parameters (discharge voltage V_d , gas pressure P , magnetic field intensity B and acceleration voltage V_{acc}). The magnetic field is collimated and intensifies the plasma that enhances the extracted beam current. The obtained cold cathode ion source can be used in different applications like surface etching, surface modification and deposition due to its long life and compactness.

Keywords: Plasma, Cold cathode, Ion beam, Discharge, Acceleration

1 Introduction

The ion source is the most important part in the ion beam system. For this reason, continuous developments in the design of ion source are needed to meet the required applications. Broad beams extracted from cold cathode ion source with uniform current distributions have an extensive utilization in a great variety of research and technology applications^{1,2}.

Cold cathode ion source are used in various applications such as metals deposition, surface cleaning, surface etching and surface modification³⁻⁷. The cold cathode is characterized by its long life, easy instrumentation and negligible maintenance due to filamentless operation⁸. The use of extracted ion beams for deposition a wide variety of materials has been demonstrated to offer some significant and unique advantages compared to other deposition methods^{9,10}. Generally, the extracted ion beams from cold cathode ion source technique offer a number of advantages when compared to the conventional plasma techniques such as the control of ion energy, ion current density, and ion distribution width and beam direction¹¹.

The cold cathode ion source is composed of two main parts, the discharge medium and the acceleration unit¹². The discharge process is produced by the electron collisions with ions along the distance between the cathode and the anode, where the anode is surrounded by magnetic field which makes increasing in the electron path with helical motion for plasma production^{13,14}. The glow discharge constitutes an attractive source for plasma-charged particle systems due to its stability and simplicity. Therefore, for long time operation and when reactive gases are used, the hot filaments are usually replaced with cold cathode ion sources^{15,16}. The discharge characteristics of the ion source depends on different parameters like cathode material, gas pressure, applied voltage and the geometry of the discharge tube¹⁷.

Magnetic field helps the electrons to confine and increases the path between the cathode and the anode. The ions produced in the ion source are extracted along the axis of the plasma column due to the potential difference between the anode and the cathode¹⁸. For this technique, the addition of magnetic field around the anode discharge chamber increases the lifetime of the ions in the plasma which results in more successive-single ionization processes, which

*Corresponding author (E-mail: alyatta2001@yahoo.com)

increases the yields of the plasma density, consequently, a higher extracted ion beam current could be obtained¹⁹. Magnetic confinement of fast electrons leads to a creation of plasma density gradient normal to the magnetic field.²⁰

The ions beams produced from the cold cathode ion source are extracted along the axis of the plasma column due to the applied potential difference between the cathode and the anode. Different geometry of the extraction electrode was studied for extracts ion beams from the extraction electrode unit²¹. The extraction electrode unit of the constructed cold cathode ion sources is multi aperture grids for producing broad beams. This development in the constructed ion source, applied mainly in surface modifications, sputtering and etching, is capable to produce low energy ion beams with high-ion current densities²².

A cold cathode ion source was previously designed and constructed to produce focused beams²³. Therefore, the paper aims to developments of cold cathode ion source with a multi-aperture accelerating system working in low pressure to produce collimated broad beams. The discharge characteristics and ion beam extracted will be characterized and discussed by measuring the discharge current and the extracted ion beam of argon gas under the influence effect of many parameters such as accelerating voltage V_{acc} , gas pressure P , discharge voltage V_d , magnetic field intensity B and extraction- acceleration distance .

2 Experimental Details

Figure 1 shows a schematic diagram of the cold cathode ion source and its associated electrical circuit. A milliammeter is used to measure the discharge current between the anode and cathode, while the high

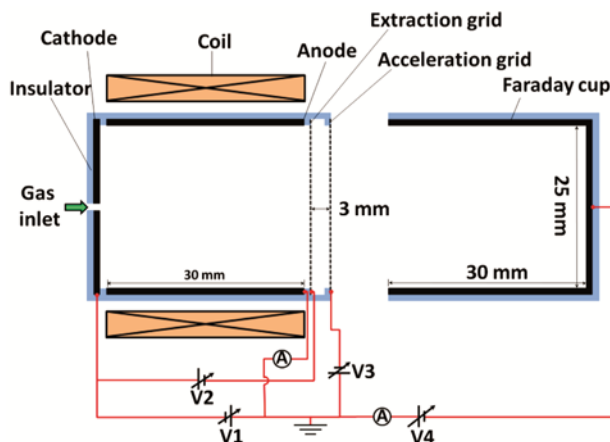


Fig. 1 – A schematic diagram of broad beam ion source.

voltage power supply is used to measure the discharge voltage between them. The stainless steel cathode is connected to earth and the collector (Faraday cup), F C, is connected to earth through microammeter which used to measure the output ion beam current that exit from the acceleration grid apertures.

A complete vacuum system is used to evacuate the ion source chamber. The working argon gas is transmitted to the ion source from a gas cylinder through a needle valve to regulate the rate of gas flow. The argon gas is admitted to the ion source through a hose fixed in flange at up side of the ion source.

The operating principle of this ion source is based on the ionization mechanism produced by primary electrons colliding with gas molecules due to a potential difference between the anode and the cathode. Therefore, high output ion beam current can be extracted axially in a direction from the discharge region to extraction part. The stainless steel extraction acceleration electrodes are separated and electrically insulated from each other by teflon rings. The output ion beam current is increases due to the applied of acceleration potential. The anode is made of stainless steel material which is featured by high ionization coefficient and it is cylinder to improve the stability of the discharge. The cathode is made of stainless which has high secondary emission coefficient.

A Faraday cup is placed at a distance 10 mm from the stainless acceleration grid. The output ion beam current is extracted from the acceleration grid. The grid is 313 exit apertures each aperture of 1 mm diameter.

A single cylindrical probe made of tungsten wire encapsulated in a glass sleeve was constructed. It is of 0.5 mm in diameter and 1 mm in length. The probe is made movable in radially and axially position to reach the desired point. The probe is placed in the beam centre at the front of the acceleration grid and at a distance ≈ 10 mm from the acceleration grid.

For measuring the ion beam profile, the electrostatic probe is connected to the ground through a negatively potential ≈ 30 V, and the ion beam is recorded through microammeter under the influence of magnetic field B , and acceleration voltage V_{acc} . A schematic diagram of the single electrostatic probe and its electrical circuit is shown in Fig. 2.

3 Results and Discussion

Figure 3 shows the discharge current I_d as a function of the discharge voltage V_d at different magnetic fields B with optimum argon gas pressure

$P=2 \times 10^{-3}$ torr. It was found that the increase in magnetic field was accompanied by an increase in the discharge current. The increase is referred to an increase in magnetic field vector parallel to anode surface, and as a consequence a reduction in the reverse electron current to the anode occurs.

The extracted ion beam I_b current increases from 0.65 to 1 mA by increasing the acceleration voltage V_{acc} from zero to 2000 V at optimum parameters, argon gas pressure $P=2 \times 10^{-3}$ torr, magnetic field $B=150$ G and discharge voltage of 900 V as shown in Fig. 4. This behavior is due to the position and shape of the ion beam extracted of the plasma, which are dependent on the value of the negative potential applied to the acceleration electrode. This fact imposes limitations on the variation of the acceleration voltage. The rise in the extracted ion beam current by increasing the acceleration voltage is due to the higher probability of extracting ions from the ion source²⁴. And may be because the ionization

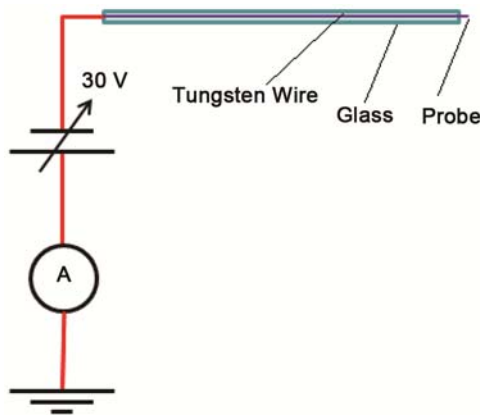


Fig. 2 – A schematic diagram of single electrostatic probe.

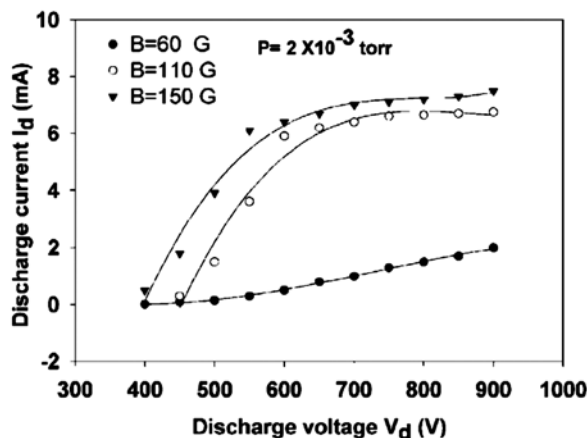


Fig. 3 – The discharge current I_d as a function of discharge voltage V_d at different magnetic field B.

probability induced due the more striking electron as well as the large ionization cross section²⁵.

Figure 5 shows the relation between the discharge current I_d and the gas pressure P with different applied discharge potentials V_d (500, 700 and 900 V) and constant magnetic field intensities B 150 G. By adjusting the discharge potential at 500 V, quite intensive glow discharge plasma is started between the cathode and the anode. With increasing the discharge potential to 700 V intensive plasma discharge takes place, and more collisions as well as semi-saturated plasma is observed by increasing the discharge voltage to 900 V. It can be seen that the discharge current relatively increases with increasing the gas pressure. This behavior may be attributed to the number of the particles that increases with the gas pressure²⁶.

The relation between the extracted argon ion beam current I_b and the gas pressure P inside the ion source at different magnetic field intensities B (60-150 G) is

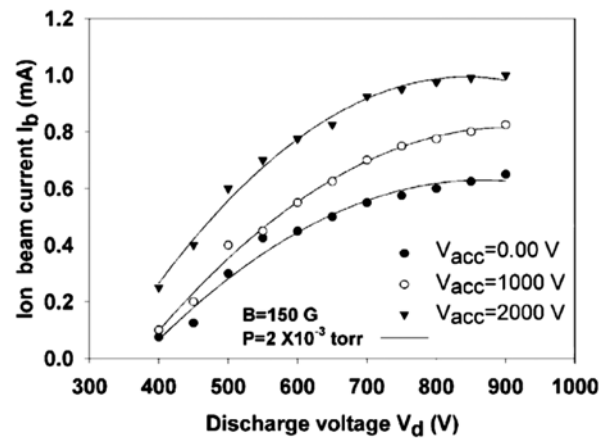


Fig. 4 – Ion current I_b as a function of discharge voltage V_d at different acceleration voltage V_{acc} .

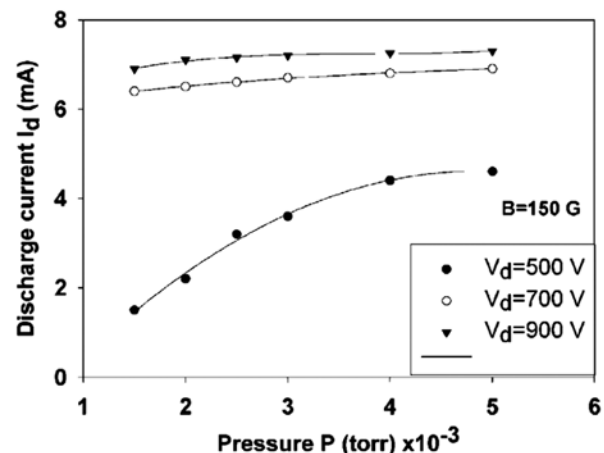


Fig. 5 – The discharge current I_d as a function of gas pressure P at different discharge voltages V_d .

shown in Fig. 6. The resultant data in Fig. 6 shows that the higher extracted ion current could be obtained at a discharge pressure of 2×10^{-3} torr. At this optimum gas pressure, 2×10^{-3} torr, the mean free path of the electron is appropriate to gain energy from the field and transfer it to the ionizing medium resulting in minimum breakdown voltage and maximum ionization cross-section²⁷. It is, also, seen that by increasing the argon gas pressure above the optimum pressure (2×10^{-3} torr), the extracted current is decreased, shown in Fig. 6. This decrease in the extracted current can be explained as the fact that the increase in the pressure inside the ion source may lead to an increase in ion scattering and hence, a beam current reduction occurs.

A relation between the discharge current I_d and the magnetic fields B for different gas pressures $P=(2, 3$ and $4) \times 10^{-3}$ torr and constant discharge voltage V_d 900 V is shown in Fig. 7. Here, the discharge current

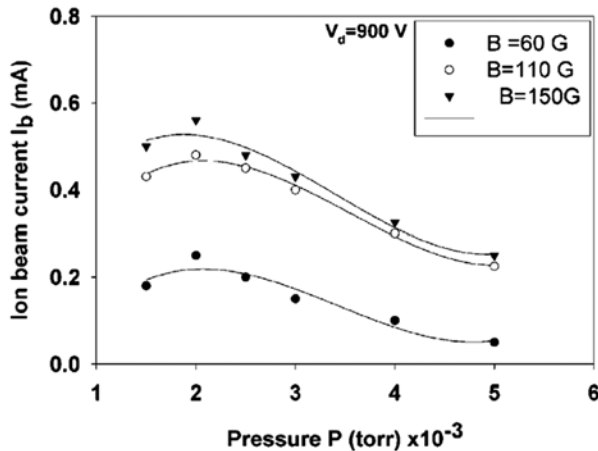


Fig. 6 – The ion beam current I_b as a function of gas pressure P at different magnetic field B .

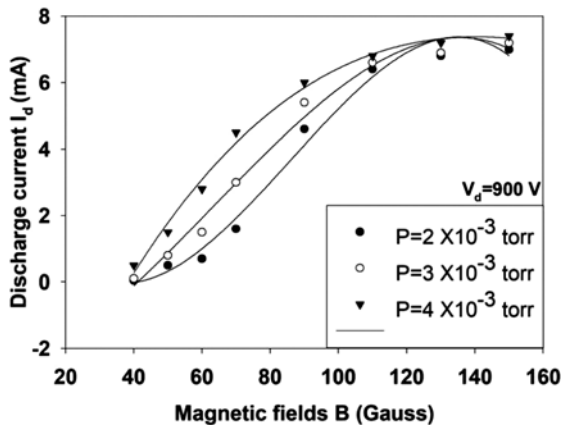


Fig. 7 – The discharge current I_d as a function of magnetic fields B at different gas pressures P .

increases with increasing the magnetic field and it seems to be semi-saturated up to 150 G. Meanwhile, the discharge current is increases in a regular manner with increasing the gas pressure ($2, 3$ & 4) $\times 10^{-3}$ torr as shown in Fig. 7. In general, as pressure increases, more gas becomes available for plasma production and the discharge current increases²⁸.

Figure 8 shows the variation of the extracted argon ion beam current as a function of the magnetic field at different gas pressures ($2-4$) $\times 10^{-3}$ torr and constant discharge voltage. The effect of the magnetic field is to collimate and intensify the plasma that enhances the extracted beam current. This means that the electrons lifetime and the capability of ionization increases, hence, it increases the plasma intensity. Also the use of the magnetic field reduces the breakdown voltage²⁹.

Figure 9 shows the influence of the acceleration voltage V_{acc} on the extracted beam current I_b at different gas pressure P with constant discharge

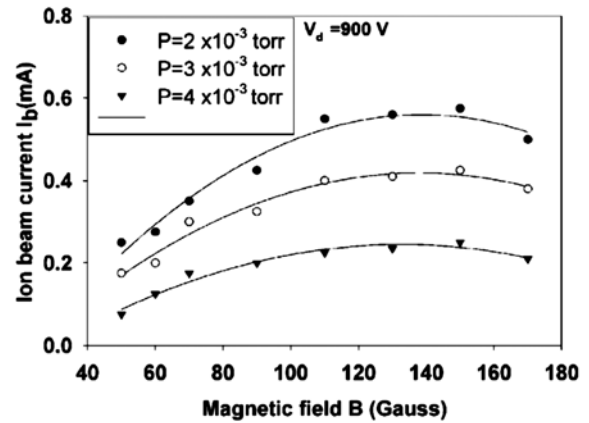


Fig. 8 – The ion beam current I_b as a function of magnetic fields B at different gas pressures P .

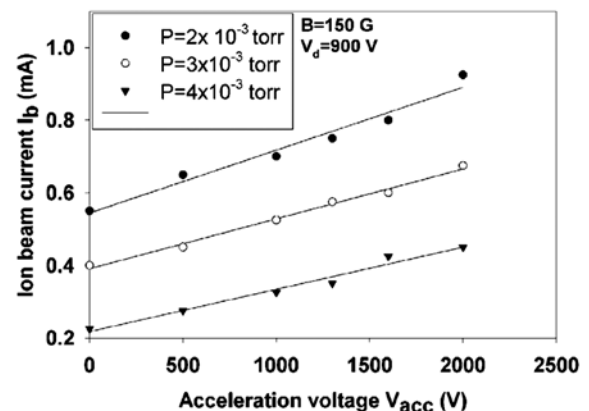


Fig. 9 – The ion current I_b as a function of acceleration voltage V_{acc} at different gas pressure P .

voltage V_d 900 V and magnetic field $B=150$ G. The increase of the acceleration voltage affects the plasma sheath voltage and thus consequently increases the extracted ion current. The extracted ion beam current density for single aperture is dependent on the acceleration voltage according to Child's law relation³⁰.

$$j = \frac{4 \epsilon_0}{9} \left(\frac{q}{m} \right)^{\frac{1}{2}} V_{acc}^{\frac{3}{2}} \frac{1}{l^2}$$

where, l is the distance between extraction and acceleration electrodes, ϵ_0 is the space permittivity= 8.85×10^{12} (F/M), V_{acc} is the acceleration voltage, q and m are the charge and the mass of ions, respectively. This implies that the extracted ion beam current is somewhat limited by ion diffusion from the discharge and is possibly limited by ion production, rather than being entirely limited by the acceleration process³¹. It is clear from Fig. 9 that the output ion beam current increased from 0.55 to 0.93 mA when the acceleration potential increased from 0 to 2000 V using argon gas pressure 2×10^{-3} torr. By increasing the gas pressure from 2×10^{-3} torr to 4×10^{-3} torr, the output ion current decreased from 0.93 to 0.45 mA at applied acceleration voltage 2000 V.

Figure 10 shows the influence of the extraction-acceleration grid distance on the extracted ion current I_b at different acceleration voltages (0, 1000 and 2000 V). It has been found that the ion beam current is higher at 3 mm space between the extraction and acceleration grids. It is interpreted as the predominant phenomenon for ionization by the

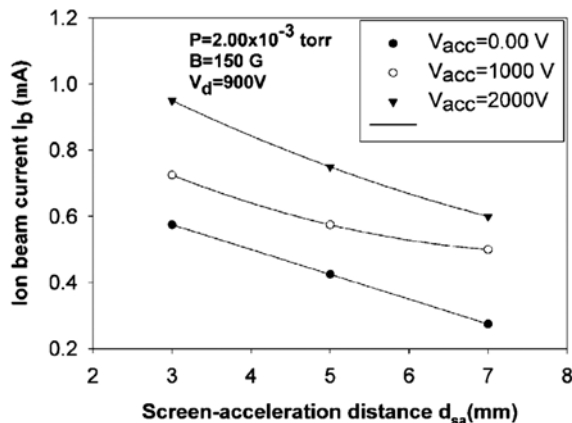


Fig. 10 – The ion beam current I_b as a function of extraction-acceleration grid distance at different acceleration voltages V_{acc} .

secondary electron emitted from the surface due to ion beam bombardment. The decrease in the electric extraction field by increasing the grids separation, will at first activate the sheath shift from inside the plasma to the whole interior with a concomitant decrease in current and divergence as shown in Fig. 10.

Figure 11 shows the relation between the discharge current I_d and the output ion beam current I_b at optimum parameters $P=2 \times 10^{-3}$ torr, $V_d=900$ V, $B=150$ G, $V_{acc}=0$ V and 3 mm distance between the extraction and acceleration grids. The measured data clearly show that an increase in the stable discharge current leads to an increase in the output ion current. When the discharge current is increased from 6.4 to 7.5 mA, the output ion beam current is increased from 0.45 to 0.65 mA.

Figure 12 shows the influence of gas pressure on ion beam current profiles using movable single

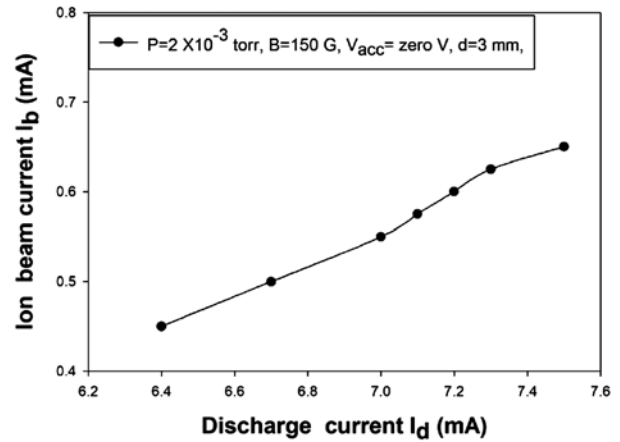


Fig. 11 – The output ion beam current I_b versus discharge current I_d using argon gas.

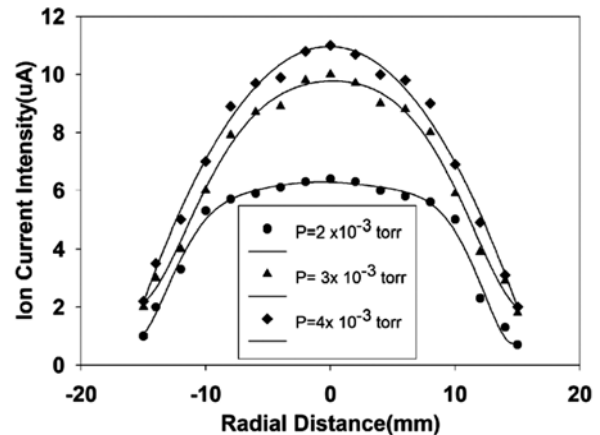


Fig. 12 – The radial distribution of the ion current intensity at different gas pressures P (parameters: $I_d=8$ mA, $V_d=900$ V, $B=150$ G, $V_{acc}=2000$ V).

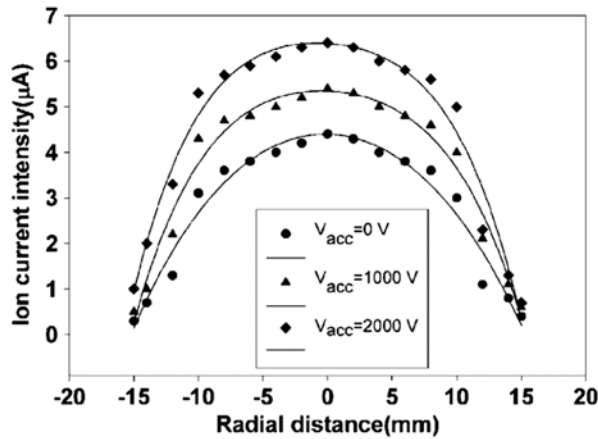


Fig. 13 – The radial distribution of the ion current intensity at different acceleration voltages V_{acc} (parameters: $I_d = 8$ mA, $V_d = 900$ V, $P = 2 \times 10^{-3}$ torr, $B = 150$ G).

cylindrical probe. In general, the beam current profile is exhibit Gaussian shape. It also shows that beam current slightly increases with pressure. At high pressure (4×10^{-3} torr), the beam diameter decreases with little distortion in intensity distribution³². Accordingly, increasing the pressures, the beam intensity correspondingly increases, up to a limiting pressure value (2×10^{-3} torr) beyond which it decreases with an indication of a decrease in gas efficiency.

The ion beam current distributions are measured at different acceleration voltages as shown in Fig. 13. The high acceleration voltage helps to focus the ion beam, then, to increase the uniformity of the ion beam. Furthermore, the beam distribution is Gaussian and the produced ion beam is broad and nearly uniform over a disc of 15 mm in diameter. It is found that the radial profile of the ion current density is nearly quite changed by the influence of acceleration voltage V_{acc} . The partial increase in ion current by increasing the acceleration voltages is due to the increases in electron energies, which are capable to ionize more gas atoms³³. This acceleration potential causes higher ion current flows towards the grid system. For good distribution ion beam current requires small grid holes, low grid distance and simultaneously high grid voltages. The grid which contains many circular holes causes the output ion beam current to be more confined.

4 Conclusions

A glow discharge cold cathode broad beam ion source has been made in NCRRT, Atomic Energy Authority, Egypt. The output ion beam current and discharge current are measured under different

parameters of the ion source such as, the discharge voltage, gas pressure, magnetic field intensity and acceleration voltage. From these measurements, it was found that, the optimum distance between the extraction and acceleration grid is 3 mm. Consequently, stable discharge current and higher output ion beam current ≈ 1 mA is obtained at this distance and optimum parameters $P = 2 \times 10^{-3}$ torr, $V_d = 900$ V, $B = 150$ G, $V_{acc} = 2000$ V. The stainless steel extraction accelerations electrodes are separated and electrically insulated from each other by teflon rings. The output ion beam current is increased due to the applied of extraction potential. The obtained cold cathode ion source is featured very simple in construction, easy to operate, working with noble and reactive gases, high efficiency with respect to lower gas consumption, long life operation. This ion source with broad beam diameter 25 mm can be used for different applications like surface modifications, etching and sputtering applications.

References

- 1 Taylor T, *Rev Sci Instr*, 63 (1992) 2507.
- 2 Rover J L, *Plasma Sour Sci Technol*, 17 (2008) 35009.
- 3 Atta A, Lotfy S, Abdelwab E, *J Appl Polym Sci*, 135 (2018) 46647.
- 4 Fawzy Y H A, Abdel-Hamid H M, El-Oker M M & Atta A, *Surf Rev Lett*, 25 (2018) 1850066.
- 5 Abdel Reheem A M, Atta A & Abdel Maksoud M I A, *Radiat Phys Chem*, 127 (2016) 269.
- 6 Atta A, Fawzy Y H, Bek A, Abdel-Hamid H M & El-Oker M M, *Nucl Instr Meth B*, 300 (2013) 46.
- 7 Abdel Reheem A M, Atta A & Afify T A, *Surf Rev Lett*, 24 (2017) 1750038.
- 8 Ensinger W, *Rev Sci Instrum*, 63 (2009) 5217.
- 9 Abdel Reheem A M, Atta A & Abd-Elmonem M S, *Surf Rev Lett*, 24 (2017) 1750031.
- 10 Abdel Reheem A M, Abdel Maksoud M I A & Ashour A H, *Radiat Phys Chem*, 125 (2016) 171.
- 11 Kaufman H R & Robinson R S, *Vacuum*, 39 (1989) 1175.
- 12 Marcus R K & Broekaert J A C, *Glow discharge plasmas in analytical spectroscopy*, John Wiley & Sons; 2003.
- 13 Lieberman M A & Lichtenberg A J, *Principles of Plasma Discharges and Materials Processing* (Wiley, NJ), 2005 535.
- 14 Godechot X & Bernardet H, *Rev Sci Instr*, 61 (1990) 2608.
- 15 Oks E M, Vizir A V & Yushkov G Y, *Rev Sci Instr*, 69 (1997) 853.
- 16 Miyamoto N, Miyabayashi K, Yamashita T & Fujisawa H, *Rev Sci Instr*, 73 (2002) 819.
- 17 Garamoon A A, Samir A, Elakshar F F & Kotp E F, *Plasma Sour Sci Technol*, 1 (2003) 417.
- 18 Marcus R K & Broekaert J A C, *Glow discharge plasmas in analytical spectroscopy*, John Wiley & Sons; 2003.
- 19 Rovey J L, *Plasma Sour Sci Technol*, 17 (2008) 35009.
- 20 Gavrilov N V & Kamenetskikh A S, *Tech Phys*, 49 (2004) 1202.
- 21 Das B K & Shyam A, *RSI*, 79 (2008) 123305.

- 22 Atta A, Abdel-Hamid H M, Fawzy Y H A & El-Oker M M, *Emer Mater Res*, 8 (2019) 354.
- 23 Saad H M, Ashour A H & Abdel-Hamid H M, *IEEE Trans Plasma Sci*, 17 (1989) 555.
- 24 Tanga D, Pua S, Huanga Q, Tonga H, Cuia X & Chub K, *Nucl Instrum Meth Phys Res B*, 257 (2007) 801.
- 25 Kuffel E, Zaengel W S & Kuffel J, *High Voltage Engineering Fundamentals*, 2nd Edn, Newnes, New Delhi, 2000.
- 26 Dazhi J, Zhonghai Y, Kunxiang X & Jingyi D, *Plasma Sci Technol*, 11 (2009) 48.
- 27 Vasil N V, Volkov N V & Sobolev S, *J Plasma Phys*, 8 (1982) 351.
- 28 Yusheng R, Jiannan W & Taoguang X, *Rev Sci Instr*, 67 (1996) 3494.
- 29 Brown S C, *Basic Data of Plasma Physics*, John Willy & Sons, New York, (1960).
- 30 Child C D, *Phys Rev*, 32 (1911) 492.
- 31 Sikharulidze G G, *Instrum Exp Tech*, 52 (2009) 249.
- 32 Zeuner M, Neumann H, Scholze F, Flamm D, Tartz M & Bigl F, *Plasma Sour Sci Technol*, 7 (1998) 252.
- 33 Hoffmann P & Heinrich F, *Vacuum*, 44 (1993) 271.